Stability Issues of Welded Pipe Containing Pulsatile Flows

Dr. Nabeel K. Abid Al-Sahib
Ass. Prof.
University of Baghdad
AL-Khwarizmi College of Eng.

ABSTRACT:

This paper deals with the dynamics and stability behavior of a welded pipe containing flowing fluid having a small harmonic component superposed. The equation of motion was derived to represent the motion of a welded pipe conveying a pulsatile flow using a tensioned Euler- Bernoulli beam theory. The finite element analysis was used to simulate the harmonic motion of a welded pipe conveying fluid. It was shown that welded pipes with clamped-clamped and clamped-pinned supports are subject to a multitude of parametric instabilities in all their modes. Stability maps are presented for parametric instabilities of welded pipe with clamped-clamped and clamped-pinned ends. It is found that the extent of the instability regions increases with flow velocity for clamped-clamped and clamped-pinned welded pipes. The most important consideration from a practical point of view is to avoid the onset of parametric resonance.

الخلاصة

يتناول البحث السلوك الديناميكي و أستقرارية الأنابيب الملحومة الناقلة للموائع ذات السرع المتغيرة. تم أشتقاق معادلة الحركة للأنابيب الملحومة الناقلة للموائع ذات السرع المتغيرة بأستخدام نظرية أويلر-برنولي للعتبات كما تم أستخدام طريقة العناصر المحددة لمماثلة الأنابيب الملحومة الناقلة للموائع التوافقية. لوحظ بأن الأنابيب الملحومة ذات حدود التثبيت مثبت-مثبت و مثبت-مدبس خاضعة لعدد من المتغيرات اللامستقرة في جميع أنماطها. تم رسم خارطة اللاأستقرارية للأنابيب الملحومة ذات حدود التثبيت الأنفة الذكر. لقد وجد بأن وجود المناطق الغير مستقرة يزداد مع زيادة سرعة جريان المائع داخل الأنابيب الملحومة ذات حدود التثبيت المذكورة أنفا.

KEYWORDS
Pustule Flow, Stability Regions, Dynamics of Pipes, Parametric Instabilities.

INTRODUCTION:

Welded pipe conveying fluid are widely used in engineering applications. One of the design challenges is to avoid pipe buckling and flutter under various operation conditions. It's clear that if the velocity of a fluid conveying in pipe is not constant, but has a harmonic fluctuation over and above a constant mean value, then the pipe experiences instability, this phenomenon is similar to a beam

subjected to a periodic axial load **[Bolotin, 1964]**. The dynamic behavior of the system strongly depends on the different kinds of boundary conditions and on the fact whether the pipe is considered to be inextensible, i.e the cross-sectional area of the pipe is constant.

Many recent researches have been carried out on the vibration of a pipe conveying fluid. Zsolt Szabo et al **[Zsolt Szabó, 1997]** studied the dynamics of a pipe containing pulsative flow, the stability analyses of the linearized systems were performed in autonomous and nonautonomous (time-periodic) case. Zsolt Szabó **[Zsolt Szabó, 2000]** investigated the dynamic behavior of a continuum inextensible pipe containing fluid flow having a velocity relative to the pipe has the same but time-periodic magnitude along the pipe at a certain time instant. Wang and Bloom **[Wang, 2001]** studied the static and dynamic instabilities of submerged and inclined concentric pipes conveying fluid, Zsolt Szabó **[Zsolt Szabó, 2003]** investigated the nonlinear dynamics of a cantilever elastic pipe that contains pulsatile flow. The equation of motion was derived by using Hamiltonian action function. He used Galerkin's technique to include only finite number of spatial modes in the solution. The stability chart of the time-varying system was computed in the space of the relative perturbation amplitude of the flow velocity and dimensionless forcing frequency using an efficient numerical method based on Chebyshev polynomials. In the near of some critical regions bifurcation diagrams were also computed which show secondary bifurcations and phase locking followed by chaotic motion.

In the industry welded pipe conveying fluid encountered, for example, in the form of exhaust pipes in engines, stacks of fuel gases, air-conditioning ducts, pipes carrying fluid (chemicals) in chemical and power plants, risers in offshore platforms, and tubes in heat exchangers and power plants. The fluid inside the pipe dynamically interacts with the pipe motion, possibly causing the pipe to vibrate.

Also, pipelines play a significant role in the economic and environmental considerations of countries. Some carry water to help irrigate desert areas; others deliver gas over vast distances, and those that carry liquid fuels often unseen as they are buried underground **[Lee and Mote, 1997]**.

In this paper an attempt to study, analytically and numerically, the effect of harmonic fluctuation of the fluid velocity on the dynamic behavior of a welded pipe conveying unsteady flow.

EQUATION OF MOTION:

The system under consideration consists of a uniform welded pipe conveying unsteady fluid sketched in Fig. (1). the pipe is initially straight, stressed, and finite length.

The equation of motion for pre-stressed single-span pipe conveying unsteady fluid as a function of the axial distance z and time t, based on beam theory is given by **[Kuiper, 2006]**:

$$EI\frac{\partial^4 y}{\partial z^4} + \left(m_f U^2 - T_{eff.}\right)\frac{\partial^2 y}{\partial z^2} + 2m_f U\frac{\partial^2 y}{\partial z \partial t} + m_f \frac{\partial U}{\partial t}\frac{\partial y}{\partial z} + m\frac{\partial^2 y}{\partial t^2} = 0 \qquad (1)$$

Where: EI is the bending stiffness of the pipe, m=mf+mp, mf is the mass of fluid per unit length, mp is the mass of the pipe per unit length, $T_{eff.} = T \pm A_i P_i$ so-called effective force, Ai is the internal cross sectional area of the pipe, Pi is the hydrostatic pressure inside the pipe, T is a prescribe axial force due to welding, and U is a fluid velocity.

The left end of the pipe is rigidly support, whereas the right end is assumed to allow no lateral displacement but to provide a restoring moment proportional to the rotation angle of the pipe. The clamped-clamped or clamped-pinned pipe is obtained from this formulation in the limit of the restoring rotational moment going to infinity or zero respectively. Thus, the boundary conditions at ends of the pipe are given as **[Paidoussis, 1998]**:

$$y(0,t) = 0 \tag{2}$$

$$\frac{\partial y(0,t)}{\partial z} = 0 \tag{3}$$

$$EI\frac{\partial^2 y(L,t)}{\partial z^2} = K_{rs}\frac{\partial y(L,t)}{\partial z} \tag{4}$$

$$y(L,t) = 0 \tag{5}$$

Where Krs is the stiffness of the rotational spring at the right end.

The statement of the problem eqs. (1) ~ (5) can be written in a non-dimensional form as follows:

$$\frac{\partial^4 \eta}{\partial \xi^4} + (\gamma + V^2)\frac{\partial^2 \eta}{\partial \xi^2} + 2\beta V\frac{\partial^2 \eta}{\partial \xi \partial \tau} + \beta\frac{\partial V}{\partial \tau}\frac{\partial \eta}{\partial \xi} + \frac{\partial^2 \eta}{\partial \tau^2} = 0 \tag{6}$$

$$\eta(0,\tau) = 0 \tag{7}$$

$$\frac{\partial \eta(0,\tau)}{\partial \xi} = 0 \tag{8}$$

$$\frac{\partial^2 \eta(1,\tau)}{\partial^2 \xi} = -K\frac{\partial \eta(1,\tau)}{\partial \xi} \tag{9}$$

$$\eta(1,\tau) = 0 \tag{10}$$

With the following dimensionless variables and parameters:

$$\eta = y/L$$
$$\xi = z/L$$
$$\tau = t\sqrt{EI/m}/L^2$$
$$V = LU\sqrt{m_f/EI}$$
$$\gamma = L^2 T_{eff.}/EI$$
$$\beta = \sqrt{\frac{m_f}{m}}$$

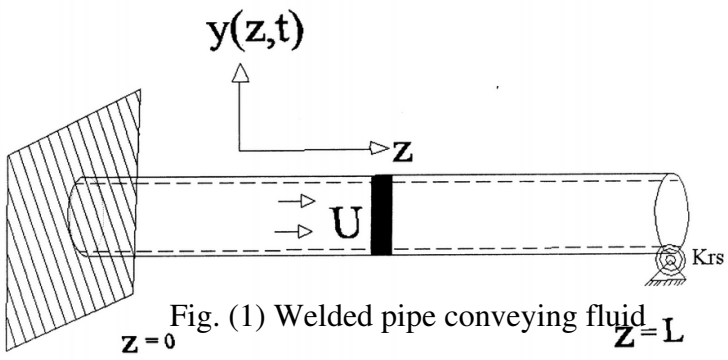

Fig. (1) Welded pipe conveying fluid

ANALYTICAL ANALYSIS:

It is clear that if a velocity of a fluid conveying in a welded pipe is not constant, but has a harmonic fluctuation under and above a constant mean value, then the pipe experiences instability.

To describe the function of this unsteady flow harmonically, Fourier series with one harmonic for the periodic velocity may be used to obtain **[Bolotin, 1964]**,

$$V = V_o[1 + \Delta Cos(w\tau)] \tag{11}$$

Where Δ is an excitation parameter, w is a non-dimensional circular frequency, and τ is a non-dimensional time.

Substituting eq. (11) into eq. (6) yields:

$$\frac{\partial^4\eta}{\partial\xi^4} + (\gamma + V_0^2\Phi^2)\frac{\partial^2\eta}{\partial\xi^2} + 2\beta V_0\Phi\frac{\partial^2\eta}{\partial\xi\partial\tau} - \beta V_0 w\Delta Sin(w\tau)\frac{\partial\eta}{\partial\xi} + \frac{\partial^2\eta}{\partial\tau^2} = 0$$

Where (12)

$$\Phi = (1 + \Delta Cos(w\tau))$$

Regions of Instabilities:

The regions of instability of eq. (12) are separated from the stable region by periodic solution with periods (T) and (2T), where ($T=2\pi/w$) hence there are two solutions of identical periods bound the region of instability, the regions enclosed by the solution having period (2T) correspond to the "primary instabilities", while the region of "secondary instabilities" are enclosed by the solution having period (T), for example, if a system with natural frequency (w_n), the primary instabilities occurs at ($w=2w_n/q$) where (q=1,3,5 …) while the secondary instability region occurs at ($w=2w_n/q$) where (q=0,2,4 …) furthermore, instabilities corresponding to (q=1 and 2) are known as the principal primary and the principal secondary instabilities respectively.

Primary Instability Regions:

To determine the region of primary instability the displacement η may be expressed as follows **[Singh, 1979]**:

$$\eta(\xi,\tau) = \sum_{q=1,3,5,\ldots} H_q(\xi)\mathrm{Sin}(\frac{1}{2}qw\tau) + R_q(\xi)\mathrm{Cos}(\frac{1}{2}qw\tau) \quad (13)$$

Where Hq and Rq are unknowns function of ξ, substituting eq. (13) into eq. (12) gives,

$$\sum_{q=1,3,5,\ldots} [\{\frac{d^4H_q}{d\xi^4} + (\gamma + V_0^2 + \frac{V_0^2\Delta^2}{2})\frac{d^2H_q}{d\xi^2} - \beta V_0 qw\frac{dR_q}{d\xi} - (\frac{q}{2})^2 w^2 H_q\}\mathrm{Sin}(\frac{qw\tau}{2}) \quad (14)$$

$$+\{\frac{d^4R_q}{d\xi^4} + (\gamma + V_0^2 + \frac{V_0^2\Delta^2}{2})\frac{d^2R_q}{d\xi^2} + \beta V_0 qw\frac{dH_q}{d\xi} - (\frac{q}{2})^2 w^2 R_q\}\mathrm{Cos}(\frac{qw\tau}{2})$$

$$+\{V_0^2\Delta\frac{d^2H_q}{d\xi^2} - \frac{\beta V_0\Delta qw}{2}\frac{dR_q}{d\xi} - \frac{\beta V_0\Delta w}{2}\frac{dR_q}{d\xi}\}\mathrm{Sin}(\frac{(q+2)w\tau}{2})$$

$$+\{V_0^2\Delta\frac{d^2R_q}{d\xi^2} + \frac{\beta V_0\Delta qw}{2}\frac{dH_q}{d\xi} + \frac{\beta V_0\Delta w}{2}\frac{dH_q}{d\xi}\}\mathrm{Cos}(\frac{(q+2)w\tau}{2})$$

$$+\{V_0^2\Delta\frac{d^2H_q}{d\xi^2} - \frac{\beta V_0\Delta qw}{2}\frac{dR_q}{d\xi} + \frac{\beta V_0\Delta w}{2}\frac{dR_q}{d\xi}\}\mathrm{Sin}(\frac{(q\quad 2)w\tau}{2})$$

$$+\{V_0^2\Delta\frac{d^2R_q}{d\xi^2} + \frac{\beta V_0\Delta qw}{2}\frac{dH_q}{d\xi}\quad\frac{\beta V_0\Delta w}{2}\frac{dH_q}{d\xi}\}\mathrm{Cos}(\frac{(q\quad 2)w\tau}{2})$$

$$+\frac{V_0^2\Delta^2}{4}\frac{d^2H_q}{d\xi^2}\{\mathrm{Sin}(\frac{(q+4)w\tau}{2}) + \mathrm{Sin}(\frac{(q\quad 4)w\tau}{2})\}$$

$$+\frac{V_0^2\Delta^2}{4}\frac{d^2R_q}{d\xi^2}\{\mathrm{Cos}(\frac{(q+4)w\tau}{2}) + \mathrm{Cos}(\frac{(q\quad 4)w\tau}{2})\}] = 0$$

The region of principal primary instability can be obtained by truncating the series in eq. (14) at (q=1), now equating the coefficients of [Sin (wτ/2)] and [Cos (wτ/2)] from both sides of eq. (14) yield,

$$\frac{d^4H_1}{d\xi^4} + (\gamma + V_0^2 + \frac{V_0^2\Delta^2}{2} - V_0^2\Delta)\frac{d^2H_1}{d\xi^2} - \frac{w^2}{4}H_1 - \beta V_0 w\frac{dR_1}{d\xi} = 0 \quad (15)$$

$$\frac{d^4R_1}{d\xi^4} + (\gamma + V_0^2 + \frac{V_0^2\Delta^2}{2} + V_0^2\Delta)\frac{d^2R_1}{d\xi^2} - \frac{w^2}{4}R_1 + \beta V_0 w\frac{dH_1}{d\xi} = 0 \quad (16)$$

Neglecting (β) results in an accuracy of the order (98%) furthermore, the effect of neglecting (β) should not be mean that the effect of fluid mass (mf) is also negligible, this is attributed to the fact that the non-dimensional flow velocity (V) and the natural frequency (w) are also function to (mf), neglecting (β) in eqs. (15) and (16) results **[Chen, 1971]**,

$$\frac{d^4H_1}{d\xi^4} + (\gamma + V_0^2 + \frac{V_0^2\Delta^2}{2} - V_0^2\Delta)\frac{d^2H_1}{d\xi^2} - \frac{w^2}{4}H_1 = 0 \quad (17)$$

$$\frac{d^4R_1}{d\xi^4} + (\gamma + V_0^2 + \frac{V_0^2\Delta^2}{2} + V_0^2\Delta)\frac{d^2R_1}{d\xi^2} - \frac{w^2}{4}R_1 = 0 \quad (18)$$

Note that eq. (17) gives the upper limit of the primary instability region, while eq. (18) represents the lower instability region; the solution of eq. (17) may be written as,

$$H_1 = E_1Sin(f_1\xi) + E_2Cos(f_1\xi) + E_3Sinh(f_2\xi) + E_4Cosh(f_2\xi) \quad (19)$$

While the solution of eq. (18),

$$R_1 = T_1Sin(k_1\xi) + T_2Cos(k_1\xi) + T_3Sinh(k_2\xi) + T_4Cosh(k_2\xi) \quad (20)$$

Where: $f_1 = \sqrt{\frac{a_1 + \sqrt{a_1^2 + w^2}}{2}}$, $f_2 = \sqrt{\frac{-a_1 + \sqrt{a_1^2 + w^2}}{2}}$

$$k_1 = \sqrt{\frac{a_2 + \sqrt{a_2^2 + w^2}}{2}}, \quad k_2 = \sqrt{\frac{-a_2 + \sqrt{a_2^2 + w^2}}{2}}$$

$$a_1 = V_0^2 + \gamma + \frac{V_0^2\Delta^2}{2} - V_0^2\Delta, \quad a_2 = V_0^2 + \gamma + \frac{V_0^2\Delta^2}{2} + V_0^2\Delta$$

And E1…E4, T1……T4 are arbitrary constants.

The upper limit can be evaluated by substituting eq. (19) into the boundary conditions eqs. (7)~(10) to give the following equation in matrix form:

$$[A_{i,j}]\{E_j\} = 0 \quad (21)$$

While the lower limit can be evaluated by substituting eq. (20) into the boundary conditions eqs. (7)~(10) yields.

$$[B_{i,j}]\{T_j\} = 0 \quad (22)$$

Both eqs. (21) and (22) are functions of many physical parameter such as (w, Δ, V_0) searching for values of any of these parameters which vanish the above determinants gives the appropriate limit of the primary region.

Secondary Instability Regions:

To determine the regions of secondary instability, the displacement ξ, is expressed as **[Singh, 1979]**,

$$\eta(\xi,\tau) = \sum_{q=0,2,4,\ldots} H_q(\xi)\mathrm{Sin}(\frac{1}{2}qw\tau) + R_q(\xi)\mathrm{Cos}(\frac{1}{2}qw\tau) \tag{23}$$

Substituting eq. (23) into eq. (12) result in eq. (14) with summation over q=0, 2, 4, … the region of the principal secondary instability can be prediction by truncated the series in the resulting equation (with q=0,2,4,…) at q=0,2 and neglecting (β) result the following equations:

$$\frac{d^4H_2}{d\xi^4} + (\gamma + V_0^2 + \frac{V_0^2\Delta^2}{2})\frac{d^2H_2}{d\xi^2} - w^2H_2 = 0 \tag{24}$$

$$\frac{d^4R_0}{d\xi^4} + (\gamma + V_0^2 + \frac{V_0^2\Delta^2}{2})\frac{d^2R_0}{d\xi^2} + V_0^2\Delta\frac{d^2R_2}{d\xi^2} = 0 \tag{25}$$

$$\frac{d^4R_2}{d\xi^4} + (\gamma + V_0^2 + \frac{V_0^2\Delta^2}{2})\frac{d^2R_2}{d\xi^2} - w^2R_2 + V_0^2\Delta\frac{d^2R_0}{d\xi^2} = 0 \tag{26}$$

Note that eq. (24) is an uncoupled differential equation related to the upper limit and may have a solution of the form:

$$H_2 = D_1\mathrm{Sin}(g_1\xi) + D_2\mathrm{Cos}(g_1\xi) + D_3\mathrm{Sinh}(g_2\xi) + D_4\mathrm{Cosh}(g_2\xi) \tag{27}$$

Where: $g_1 = \sqrt{\frac{b_1 + \sqrt{b_1^2 + 4w^2}}{2}}$, $g_2 = \sqrt{\frac{-b_1 + \sqrt{b_1^2 + 4w^2}}{2}}$

$$b_1 = V_0^2 + \gamma + \frac{V_0^2\Delta^2}{4}$$

While eqs. (25) and (26) are coupled differential equations related to the lower limit and can be solved by using the series solution as,

$$R_0 = \sum_{j=1}^{8} d_{0j}e^{\Lambda_j\xi} \tag{28}$$

And

$$R_2 = \sum_{j=1}^{8} d_{2j}e^{\Lambda_j\xi} \tag{29}$$

Where Λj's are the roots of the polynomial

$$\Lambda^4 + (\gamma + v_0^2 + \frac{v_0^2\Delta^2}{2})\Lambda^2 \qquad v_0^2\Delta\Lambda^2$$

$$2v_0^2\Delta\Lambda^2 \qquad \Lambda^4 + (\gamma + v_0^2 + \frac{3v_0^2\Delta^2}{4})\Lambda^2 - w^2 \tag{30}$$

Note that d0j's and d2j's are related to each other by,

$$d_{0j} = \frac{v_0^2\Delta\Lambda_j^2}{[\Lambda_j^4 + (\gamma + v_0^2 + \frac{v_0^2\Delta^2}{2})\Lambda_j^2]} d_{2j}$$

There are two limits which bound the principal secondary instability regions, the upper and lower limits; the upper limit can be evaluated by substituting eq. (27) into the boundary conditions equations eqs. (7)~ (10) Which gives,

$$[A_{i,j}]\{D_j\} = 0 \tag{31}$$

While the lower limit can be evaluated by substituting eqs. (28)& (29) into the boundary conditions eqs. (7)~ (10) yields,

$$[B_{i,j}]\{d_j\} = 0 \tag{32}$$

Both equations (31) and (32) are functions of many physical parameters such as (μ, w, Δ, and V) searching for values of any of these parameters which vanishing the above determinants gives the appropriate limit of the secondary region.

FINITE ELEMENT MODELING PROCEDURE:

The FE analysis was carried out using a general purpose FE package ANSYS V9.0. The approach is divided into five parts: thermal analysis, coupled field thermal-structure analysis, computational fluid dynamics (CFD), coupled field fluid-structure analysis, and modal analysis.

A non- linear transient thermal analysis was conducted first to obtain the global temperature history generated during and after welding process. A stress analysis was then developed with the temperatures obtained from the thermal analysis used as loading to the stress model.

The solutions of the governing Navier-Stokes equations for the axisymmetric geometries modeled are obtained using ANSYS FLOTRAN analysis. The governing flow equations are discretized in space according to the spectral element method. Spectral elements combine high order accuracy with the geometric flexibility of low-order finite element methods. The computational domain is divided into a number of non-degenerate spectral elements within which all information on geometry, flow

initial and boundary conditions and solutions is approximated by high order polynomial expansions. A local mesh is constructed within each element, and points on this mesh are used as interpolate points for the expansion of all dependent variables. All the simulations were performed with no-slip (zero velocity) conditions at all walls and zero pressure at the flow outlet.

The coupled field fluid-structure analysis solved the equations for the fluid and solid domains independently of each other. It transfers fluid forces and solid displacements, velocities across the fluid-solid interface. The algorithm continues to loop through the solid and fluid analyses until convergence is reached for the time step (or until the maximum number of stagger iterations is reached). Convergence in the stagger loop is based on the quantities being transferred at the fluid-solid interface.

Finally used modal analysis to determine the vibration characteristics (natural frequencies and mode shapes) of a welded pipe conveying fluid. The natural frequencies and mode shapes are important parameters in the design of a structure for dynamic loading conditions.

RESULTS AND DISCUSSIONS:

Study the stability issues for particular single span ASTM214-71 mild steel welded pipe system with (1 m) length, (50.8 mm) outer diameter, (1.5 mm) thickness. The welded pipe was formed by joining two (0.5 m) pipes by fusion arc welding with a current of 30 A and voltage equal 460 volt using an electrode type E7010-G to make a straight pipe 1m length with welding on its mid span.; the welding procedure was modeled as a single pass in this analysis.

The analytical analysis is performed using Matlab V6.5 software to determine the limits of primary and secondary instability regions. The program was developed to be used for any specified pipe dimensions, length, pipe material stiffness, different flow velocities, and welding specifications. The FE analysis is performed using ANSYS V9.0 software. The parameters used in the calculations are listed in table (1).

Table (1) Parameters used in the calculation

EI	**$1.4122*10^4$**	**Nm^2**
m_f	**1.795**	**Kg/m**
m	**3.608**	**Kg/m**
R	**25.4**	**mm**
$T_{eff.}$	**$3.0243*10^5$**	**N**
L	**1**	**m**
ρ_f	**1000**	**Kg/m^3**
β	**3.264**	

Clamped-Clamped Welded Pipe:

Fig. (2) Shows the regions of parametric instability in the range $0.5 < w/ w_{01} < 6.0$ for a clamped-clamped welded pipe ($V_0 = 2$), where w_{01} is the first mode natural frequency at zero flow. If instead of w/ w01, the ordinate w/ w_n had been utilized, where w_n is the actual natural frequency for the mode concerned at $V_0=2$, then the principal primary regions of all the modes would begin at w/ $w_n=2$, the second primary region at $w/w_n=2/3$, the principal secondary region at w/ $w_n=1$, and so on.

With the ordinate used here, associated with the first mode are:

1- The principal primary region beginning at w/ w_{01}= 1.8.
2- The principal secondary at w/ w_{01}=0.9.
3- The secondary primary region beginning at w/ w_{01}=0.6.

Similarly, associated with the second mode, the corresponding regions begin at w/ w_{01}= 5.1, 2.6, and 1.7, respectively. Associated with the third mode are the (1) principal secondary region beginning at w/ w_{01}= 5.1, and second primary region at w/ w_{01}=3.4.

Fig. (3) Shows the effect of flow velocity on the principal regions of instability associated with the first mode of a clamped-clamped welded pipe. It is noted that as the flow velocity increases the regions of instability are displaced downwards, which reflects the decrease of the first mode frequency with flow. It is also noted that the regions of instability become broader with increasing flow.

Fig. (4) Shows the effect of β on parametric instabilities. It is seen that with increasing β the regions of instability become broader and displaced downwards, which reflects the lowering of the natural frequencies as β increases for this particular flow velocity.

Clamped-Pinned Welded Pipe:

Fig. (5) Shows the parametric instability regions for a clamped-pinned welded pipe for V_0=4.5, 5.5, 6 in the range w/w02 < 2.4. the large regions of instability in the middle of the figure are the principal primary regions associated with the second mode, while at the bottom is a principal secondary region which occurs for V_0=6 only. The small regions at the top are principal secondary regions associated with the third mode.

Figures (6a, b) show, respectively, the primary and secondary instability regions, for the range of frequencies shown, of a welded pipe. The three uppermost regions of instability in figure (6a), for V_0=6, 7.5, 8 and 9, are principal primary regions associated with the third mode, while the two large regions in the middle, for V_0=8 and 9, are a mixture of principal primary regions associated with the second and third modes.

Finally, the smaller regions at the bottom of figure (6b) may similarly be divided into the following two groups: (i) the regions for V_0=6, 7.5, and 8 are mixtures of principal primary regions associated with the second mode and of second primary regions associated with the third mode, (ii) the regions for V_0=8 and 9 are mixtures of second primary regions associated with the second and third modes. This fusion of the regions of instability is shown particularly well in the cases of v0=8 and 9, where each of the regions is formed of two interlinked distinct zones, the upper of which is related to the second mode and the lower to the third mode.

In figure (6b) the upper region (V_0=6) is the principal secondary one associated with third mode, while the remaining regions are all mixtures of principal secondary regions associated with the second and third modes. The upper areas of the latter are associated with the third mode and the lower areas with the second, except for V_0=8 where no such distinction may be made.

It would be of interest to compare the results of dynamic stability obtained for a pipe conveying unsteady flow without welding by Chen **[Chen, 1971]**. We can see that the effect of welding is to reduce the range of beginning the principal primary, principal secondary, and second primary regions of instability for clamped-clamped and clamped-pinned boundary conditions.

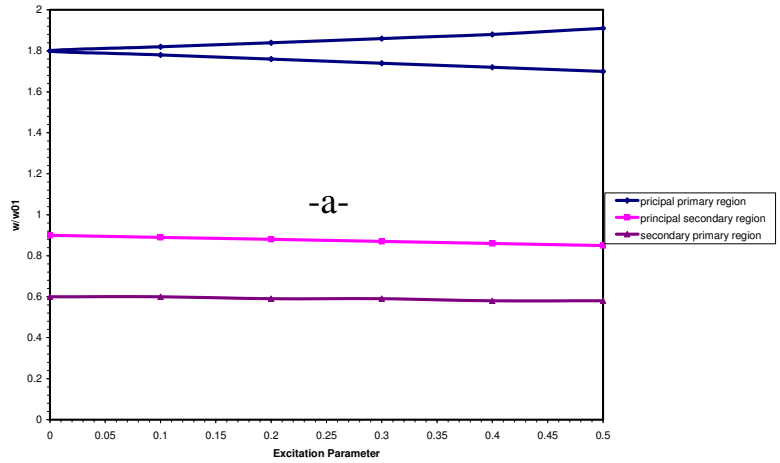
-a-
w/w01
Excitation Parameter
pricipal primary region
principal secondary region
secondary primary region

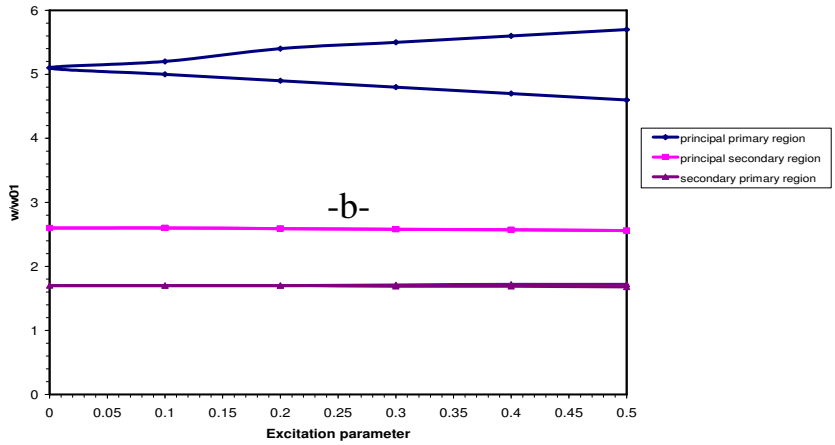
-b-
w/w01
Excitation parameter
principal primary region
principal secondary region
secondary primary region

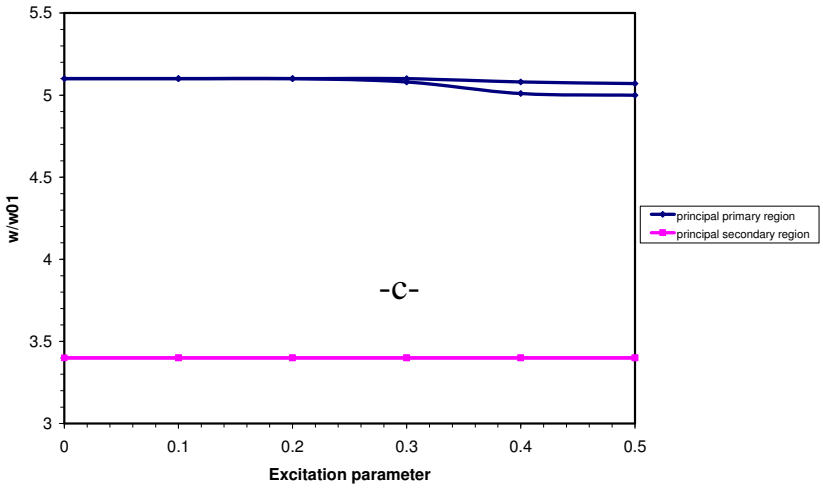
-c-
w/w01
Excitation parameter
principal primary region
principal secondary region

Fig. (2) Parametric instability boundaries for a clamped-clamped welded pipe (V_0=2). The system is unstable within the triangular regions
a- First mode b- Second mode c- Third mode

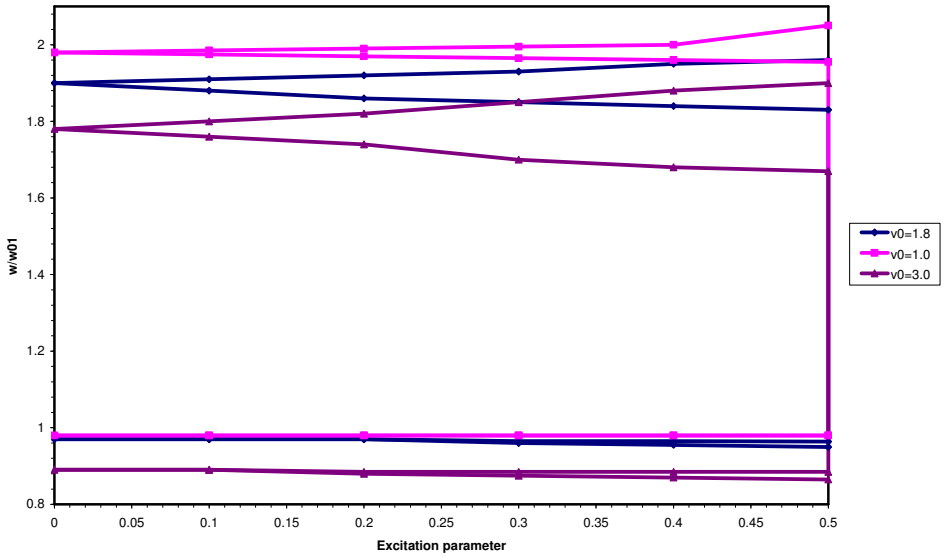

Fig. (3) The effect of flow velocity, V_0, on the principal instabilities associated with the first mode of a clamped-clamped welded pipe, for three values of V_0

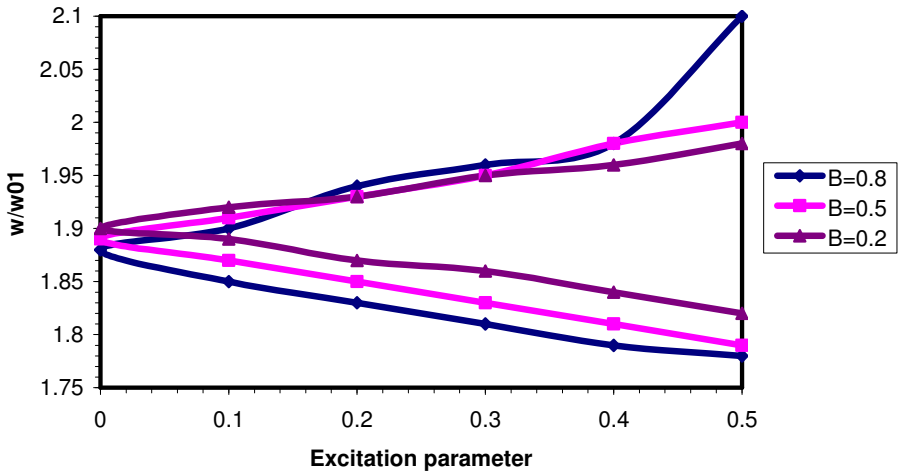

Fig. (4) The effect of β on parametric instabilities

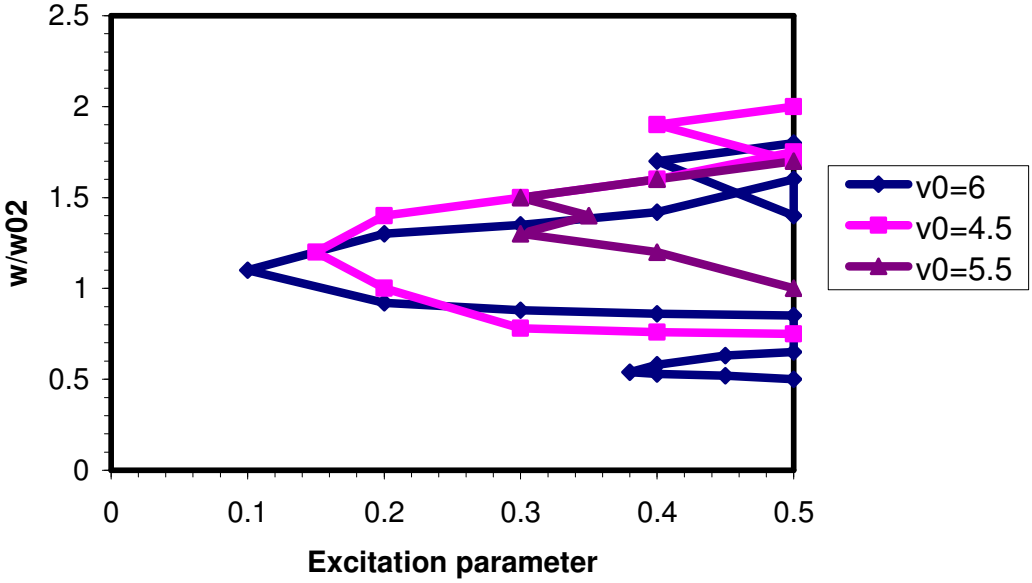

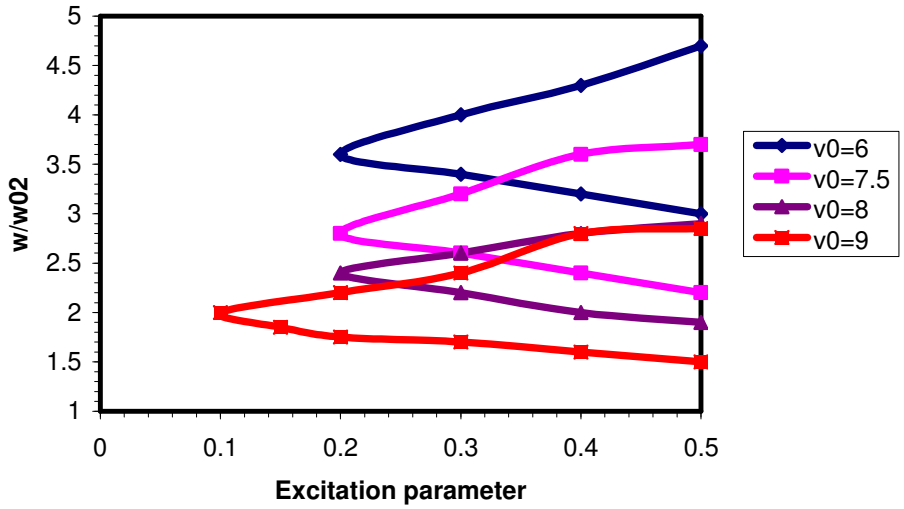

Fig. (5) Parametric instability boundaries for a clamped-pinned welded pipe

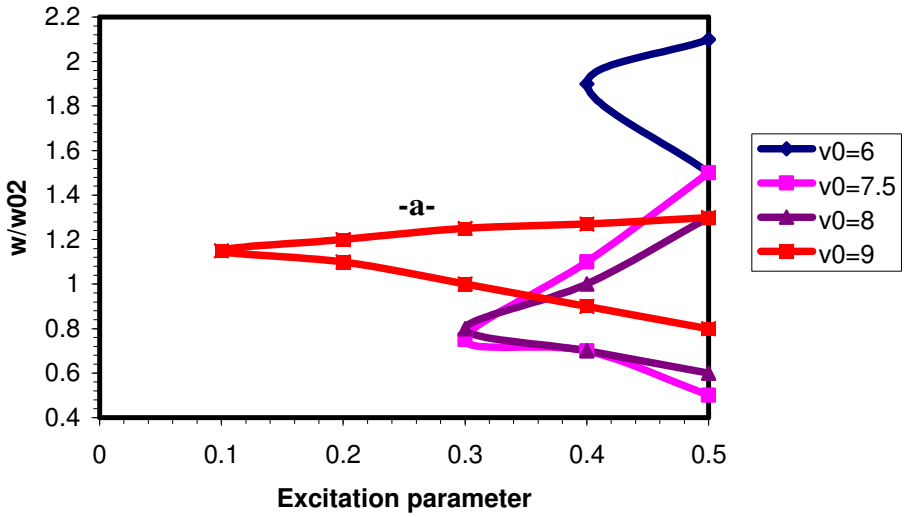

-b Fig. (6) Parametric instability boundaries for a clamped-pinned welded pipe
a- Primary instability regions b- Secondary instability regions

CONCLUSIONS

Analytical and finite element analyses are used to determine the regions of instability of a welded pipe conveying pulsatile flow with clamped-clamped and clamped-pinned boundary conditions. It was shown that these welded pipes are subjected to a multitude of parametric instabilities in all their modes. It was shown also that the pulsating flow in a welded pipe can cause parametric resonance, resembling a column subjected to periodic axial loads. The onset of instability in engineering systems, such as welded pipes could be catastrophic. The most important consideration from a practical point of view is to avoid the onset of parametric resonance.

REFERENCES

Bolotin V. V., "The Dynamic Stability of Elastic System", San Francisco Hoiden Day Inc. 1964.

Chen S. S., "Dynamic Stability of Tube Conveying Fluid", Journal of the Engineering Mechanics Division Proceeding of the American Society of Civil Engineering, pp. 1469-1485, 1971.

Kuiper G. L., and Metrikine A. V., " On Stability of a Clamped-Pinned Pipe Conveying Fluid", Heron, Vol. 49, No. 3, pp. 211-231, 2004.

Lee S. Y., and Mote C. D., "A Generalized Treatment of the Energetic of Translating Continua, Part I: Strings and Tensioned Pipes", Journal of Sound and Vibration 204, pp. 717-734, 1997.

Lee S. Y., and Mote C. D., "A Generalized Treatment of the Energetic of Translating Continua, Part II: Beams and Fluid Conveying Pipes", Journal of Sound and Vibration 204, pp. 735-753, 1997.

Paidoussis M. P., "Fluid-Structure Interactions: Slender Structures and Axial Flow", Vol.1, Academic Press, London, 1998.

Singh K., and Malik A. K., "Parametric Instabilities of Periodically Supported Pipe Conveying Fluid", Journal of Sound and Vibration, Vol.62, No. 3, pp. 379-397, 1979.

Wang X., and Bloom F., "Stability Issues of Concentric Pipes Containing Steady and Pulsatile Flows", Journal of Fluids and Structures< 15, 1137-1152, 2001.

Zsolt Szabó, Sinha S. C., and Gabor Stepan, "Dynamics of Pipes Containing Pulsative Flow", ASME Design Engineering Technical Conferences, September 14-17, Sacramento, California, 1997.

Zsolt Szabó, "Bifurcation Analysis of a Pipe Containing Pulsatile Flow", PERIODICA POLYTECHNICA SER. MECH.ENG. VOL.44, NO.1, 149-160, 2000.

Zsolt Szabó, " Nonlinear Analysis of a Cantilever Pipe Containing Pulsatile Flow", Journal of Meccanica, Springer Netherlands, Volume 38, Number 1,pp. 163-174, January, 2003.